Supporting Information

Insights into Interfacial Mechanisms: $CsPbBr_3$ Nanocrystals as Sustainable Photocatalysts for Primary Amine Oxidation

Monika Ahlawat and Vishal Govind Rao*

Department of Chemistry, Indian Institute of Technology Kanpur, Kanpur, 208016, Uttar Pradesh, India

Corresponding Author

* Vishal Govind Rao, Department of Chemistry, Indian Institute of Technology Kanpur, Kanpur, 208016, UP, India; orcid.org/0000-0003-1205-3006; E-mail: vgrao@iitk.ac.in

S1. Materials

Cesium carbonate (Cs_2CO_3, 99%), lead bromide ($PbBr_2$, ≥ 98%), octadecene (ODE, 90%), oleic acid (OAc, 90%) oleylamine (OAm, 70%), acetone (Thermofisher), benzylamine (Sigma Aldrich), 4-methoxy benzylamine (TCI), $CDCl_3$ (Eurisotop), 1,3,5-trimethoxybenzene (Mesitylene, Sigma Aldrich), Proline (Avra) 5,5-Dimethyl-1-pyrroline N-oxide (DMPO, ≥98.0%), Toluene (99.8%), 4-(methylthio)benzylamine (Sigma Aldrich).

Note: All the reagents were used as procured without any further purification.

S2. Characterization

The absorption and steady-state photoluminescence (PL) spectra of $CsPbBr_3$ NCs were acquired using a UV-Vis-NIR spectrophotometer (JASCO V770) and FluoroMax+, Horiba Scientific. Further, the structural characterization of $CsPbBr_3$ NCs was carried out with transmission electron microscopy, TEM (FEI- Tecnai G^2 12 Twin TEM 120 kV). The size distribution and lattice *d*-spacing were estimated using ImageJ software. All one and two-dimensional Nuclear magnetic resonance (NMR) measurements were performed on the JEOL ECZ-500 MHz NMR instrument. ^1H spectrum was acquired with a spectral width set to 10 ppm and a relaxation delay time of 2 s. The mixing time for the 2D Nuclear Overhauser Effect Spectroscopy (NOESY) spectrum was set to 300 ms with a spectral width of 10 ppm. Powder X-ray diffraction pattern (PXRD) study was performed on PANalytical X'Pert by PANalytical. Electron paramagnetic resonance (EPR) spectra were acquired from Bruker's EMX EPR spectrometer. Gas chromatography-mass spectrometry (GC-MS) was performed on Agilent 8890 GC and 5977B GC/MSD systems. Fourier-transformed infrared spectrum (FTIR) was acquired using BRUKER ALPHA-II (ECO-ATR mode). Elemental analysis of $CsPbBr_3$ NCs was done through X-ray photoelectron spectroscopy (XPS) on PHI 5000 Versaprobe-II, FEI Inc., Japan, equipped with a monochromatic Al Kα (1486.6 eV) radiation source. We performed the photocatalytic reactions using a visible range Fibre-Coupled Illuminator, OSL2 from ThorLabs.

S3. Synthesis of $CsPbBr_3$ NCs

$CsPbBr_3$ NCs were synthesized following an earlier report with slight modifications.[1] Firstly, we prepared Cs-oleate by adding 40.7 mg of Cs_2CO_3 to 2 mL ODE in a 50 ml 3-neck RB flask, followed by 125 μL of OA. The above mixture was then heated to 120 °C for 1 h under N_2 purging. The temperature was then increased to 150 °C until the Cs_2CO_3 was completely dissolved to form a clear yellow-brown Cs-oleate solution. In another RB flask, 138 mg of $PbBr_2$ was added to 10 mL ODE heated at 100 °C. 1 mL of OAm and OAc each was further added to the mixture and the temperature increased to 120 °C for ~ 1 h with N_2 purging. The mixture was allowed to heat while stirring until the $PbBr_2$ completely dissolved to form a clear solution. The temperature was further increased to 160 °C with continuous N_2 purging. The as-prepared Cs-oleate solution (0.8 m) was quickly injected into the reaction mixture, and the reaction was immediately quenched in an ice water bath. The crude solution was then precipitated using acetone as an anti-solvent and centrifuged at 12000 rpm. The supernatant was discarded, and the pellet was redispersed in toluene. The solution was again centrifuged at 4000 rpm, and the supernatant was stored for further use.

S4. Estimation of Concentration of $CsPbBr_3$ NCs: The concentration of $CsPbBr_3$ NCs was calculated using intrinsic and molar absorption coefficients, as reported earlier.[2,3] The following equation was used to derive molar extinction coefficient (ε) of $CsPbBr_3$ NCs in terms of intrinsic absorption coefficient (μ_i).

$$\varepsilon = \frac{N_a\, V_{NC}}{ln10}\, \mu_i \qquad (1)$$

Where, N_a = Avogadro constant

V_{NC} = NC volume (as extracted from TEM data analysis)

μ_i (at 335 nm) = 1.98×10^5 cm^{-1}

Further, we applied Beer Lambert's law (at 335 nm absorption wavelength) to estimate the concentration (Molar) of $CsPbBr_3$ NCs

$$A_{335} = \varepsilon_{335}\, CL \qquad (2)$$

A_{335} = absorbance of $CsPbBr_3$ NCs dispersion at 335 nm

L = optical path length (1cm), and

C is the concentration to be calculated.

S5. Spectroscopic characterization of $CsPbBr_3$ NCs

In the absorbance and steady-state PL spectrum, the colloidal solution of $CsPbBr_3$ NCs in toluene displayed a prominent excitonic feature at 507 nm. Examination of the TEM image (inset of Figure S1a) revealed that the NCs possessed an approximate size of 12 nm. The PXRD spectrum unveiled the cubic phase crystal structure of $CsPbBr_3$ NCs (Figure S1b). Significantly, we verified the existence of OAm and OAc as a ligand shell on the NC's surface NMR spectroscopic analysis (Figure S1c), which contributes to the colloidal stability of the $CsPbBr_3$ NCs.

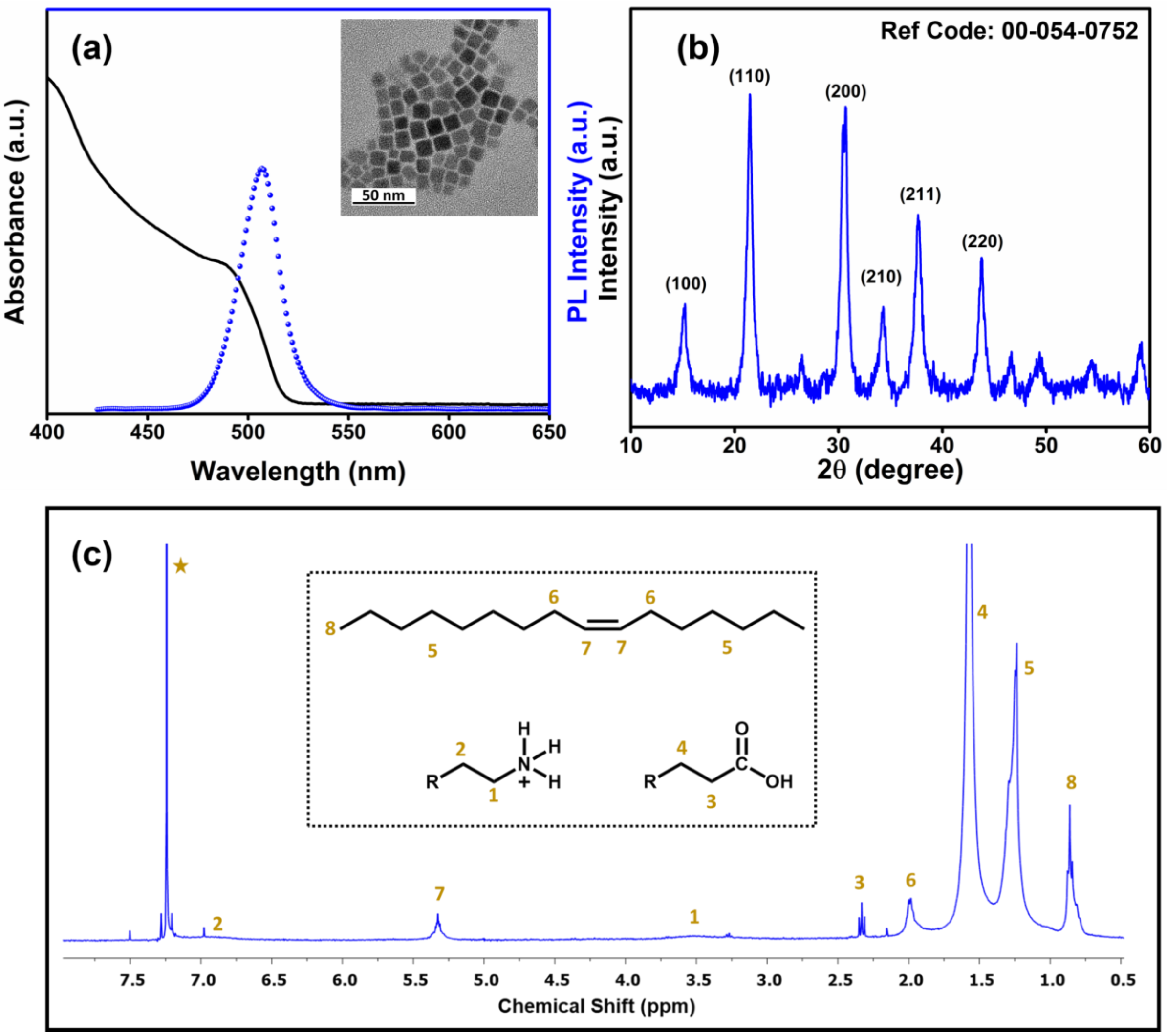

Figure S1. (a) Absorbance and PL spectrum of the colloidal solution containing $CsPbBr_3$ NCs in toluene. Inset: TEM image of $CsPbBr_3$ NCs. (b) PXRD spectrum of $CsPbBr_3$ NCs. (c) ^1H NMR spectrum of $CsPbBr_3$ NCs acquired in $CDCl_3$. The chemical shift values are indexed with their corresponding protons in OAm and OAc.

S6. Photocatalytic conversion of benzylamine to N-benzylidenebenzylamine

The catalytic reaction was carried out in a 2 ml reaction vessel. A benzylamine solution (60 µL, 1M) was added to a colloidal solution of $CsPbBr_3$ NCs (~ 6 µM, 0.4 mL) in toluene. The reaction vessel was filled with O_2 and pressure was maintained using O_2 balloon. The reaction mixture was allowed to stir for 10 min to equilibrate over the catalyst surface. Later, the reaction mixture was exposed to visible light for 10 h with constant stirring (keeping the outside temperature 25 °C). The intensity of light falling on reaction vessel was measured to be ~ 450 $mWcm^{-2}$ (except for the light intensity dependence control experiments). After completion of the reaction the crude solution was dried under vacuum and the product yield was determined by ^1H NMR spectroscopic technique using mesitylene (1,3,5-trimethoxybenzene) as internal standard. All the NMR measurements were performed in $CDCl_3$ solvent. For the GC-MS analysis, the dried crude reaction mixture was separated with the addition of ethyl-acetate (acting as antisolvent).

S7. ^1H NMR analysis of standard photocatalytic reaction and other control experiments

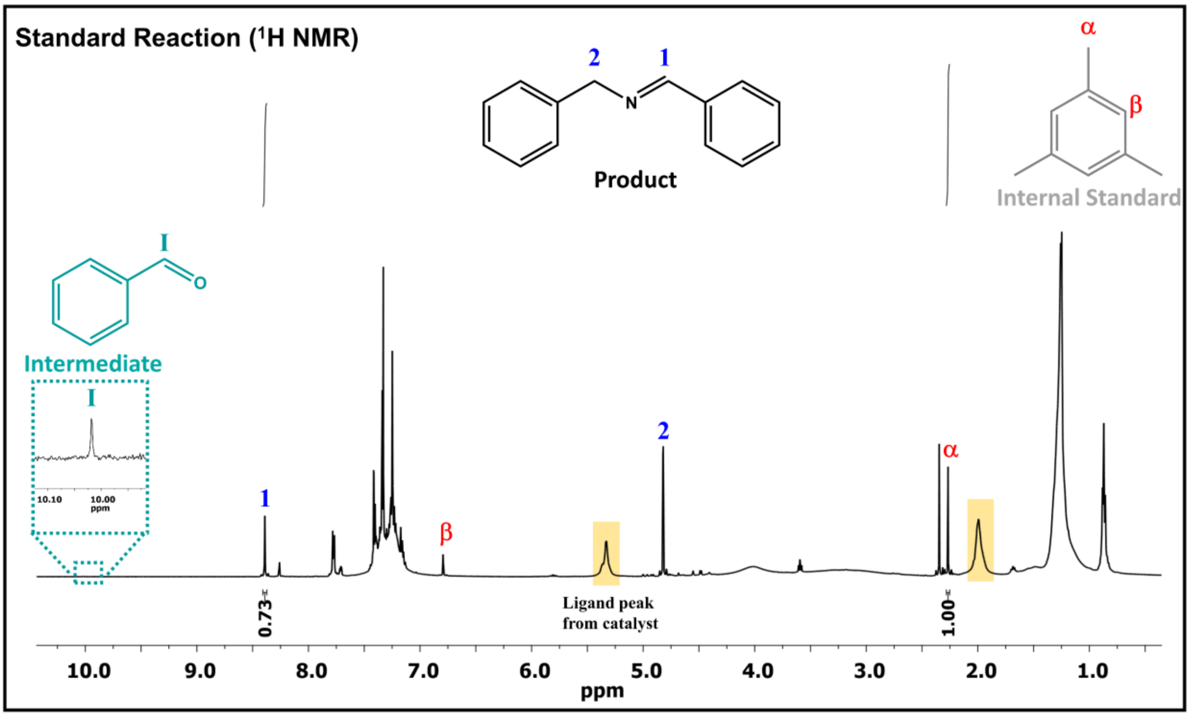

Figure S2. ^1H NMR analysis of the standard reaction (crude) in $CDCl_3$. Mesitylene was used as internal standard for quantification of product. Aldehydic proton (I) highlight the formation of benzaldehyde in the reaction mixture which has been considered as an intermediate for imine formation reaction.

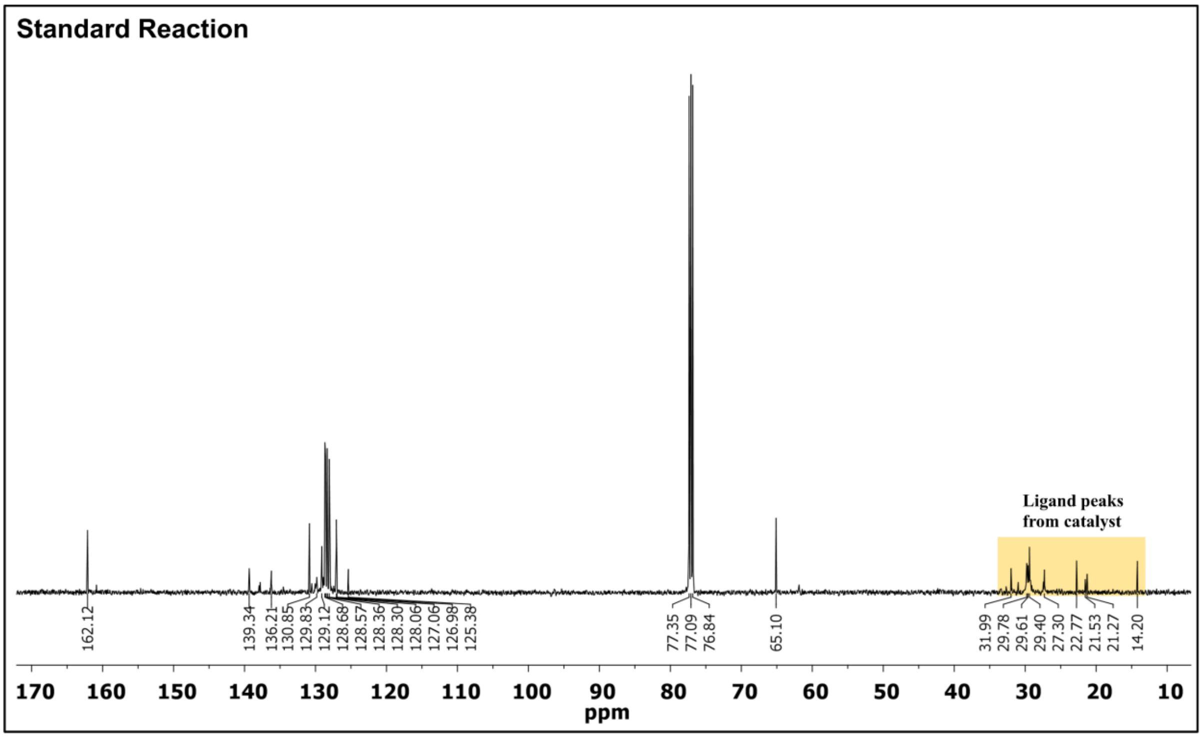

Figure S3. ^{13}C NMR spectrum of standard reaction mixture (crude) in $CDCl_3$.

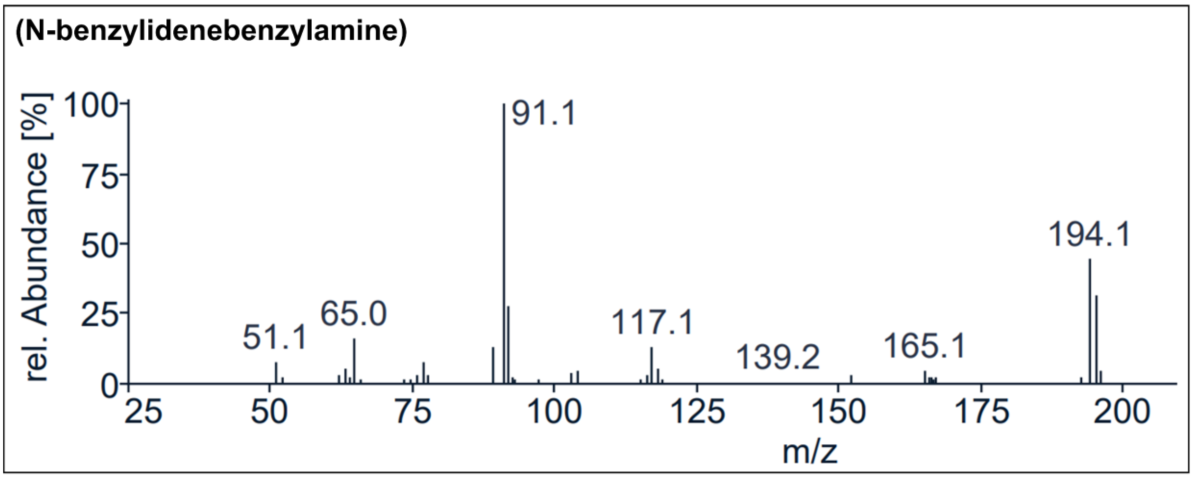

Figure S4. Mass spectrum of the product, N-benzylidenebenzylamine obtained from GC-MS analysis.

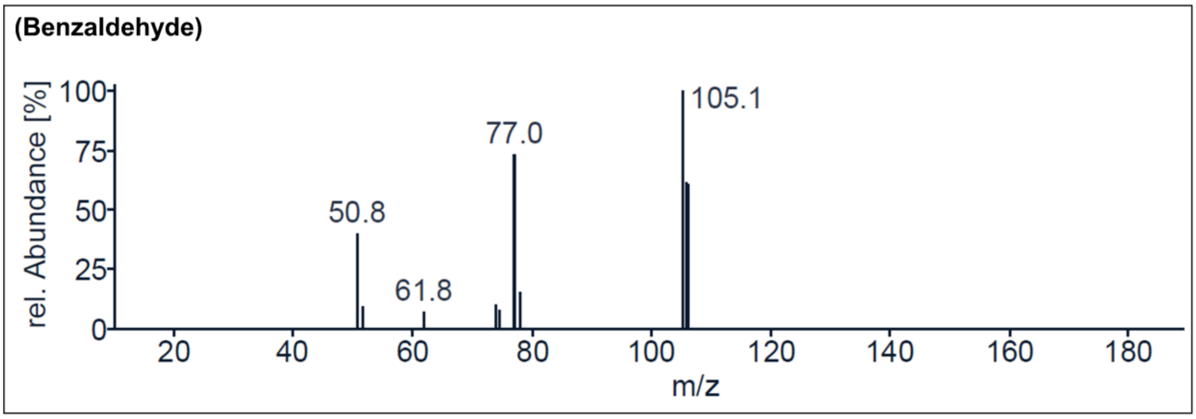

Figure S5. Mass spectrum of the intermediate (benzaldehyde) obtained from GC-MS analysis.

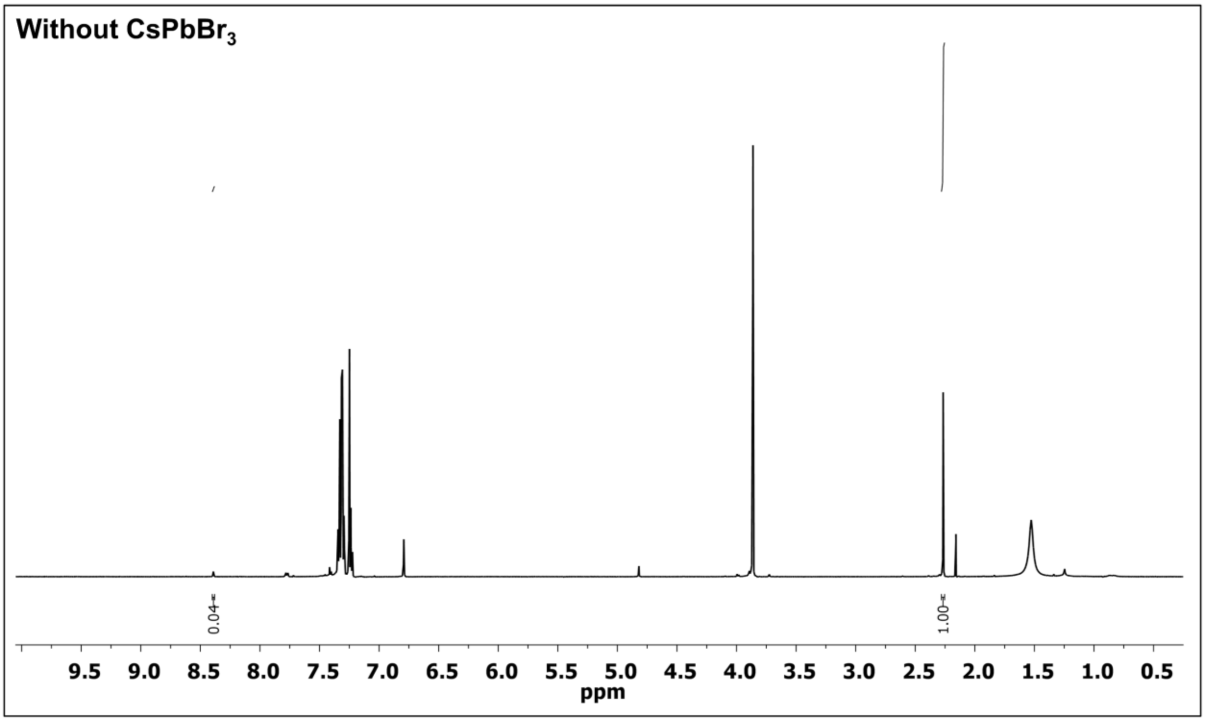

Figure S6. ^{1}H NMR spectrum of control experiment performed in absence $CsPbBr_3$ NCs (pure toluene was used as solvent) keeping the other reaction conditions unchanged.

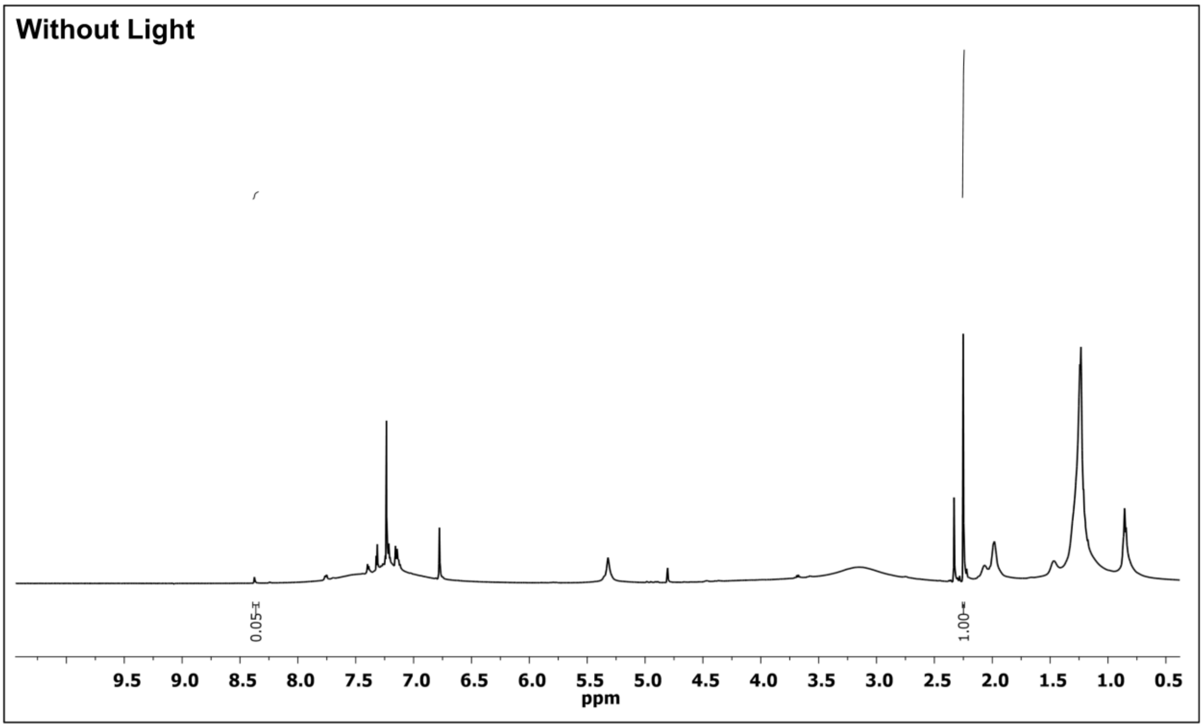

Figure S7. ^{1}H NMR spectrum of control experiment performed in absence of light irradiation keeping the other reaction conditions unchanged.

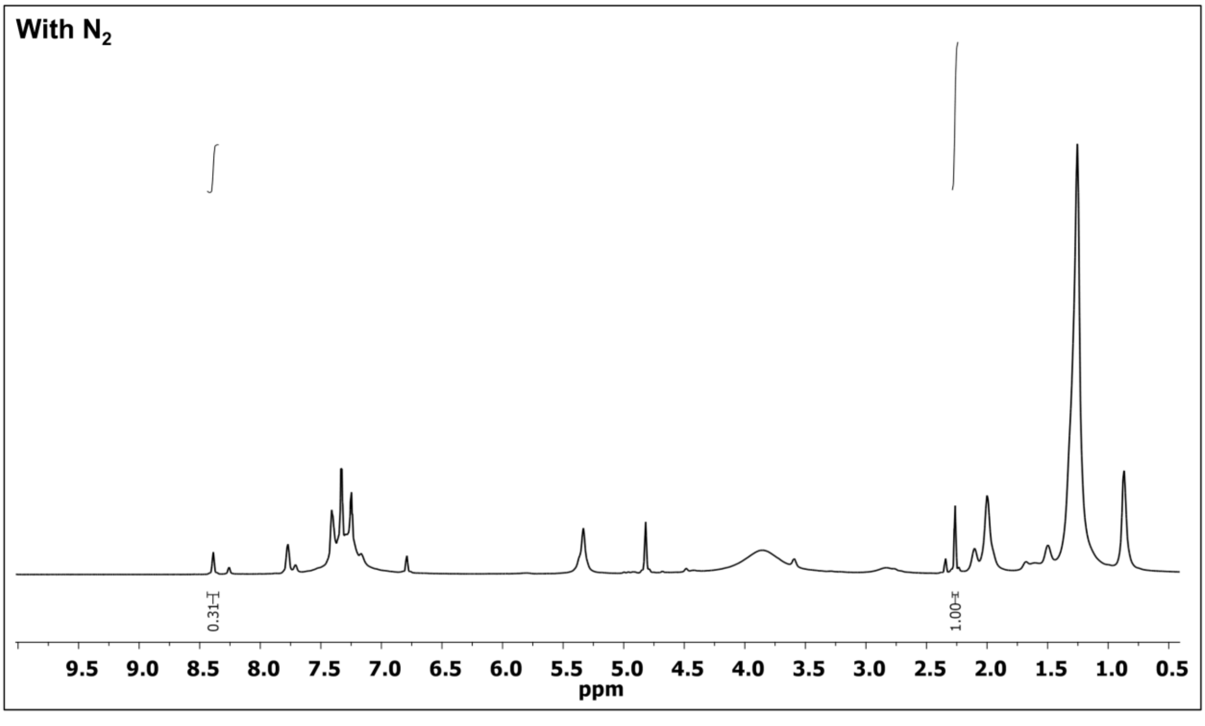

Figure S8. ^{1}H NMR spectrum of control experiment performed in absence in absence of O_2 (maintaining N_2 pressure in the reaction vessel using balloon) keeping the other reaction conditions unchanged.

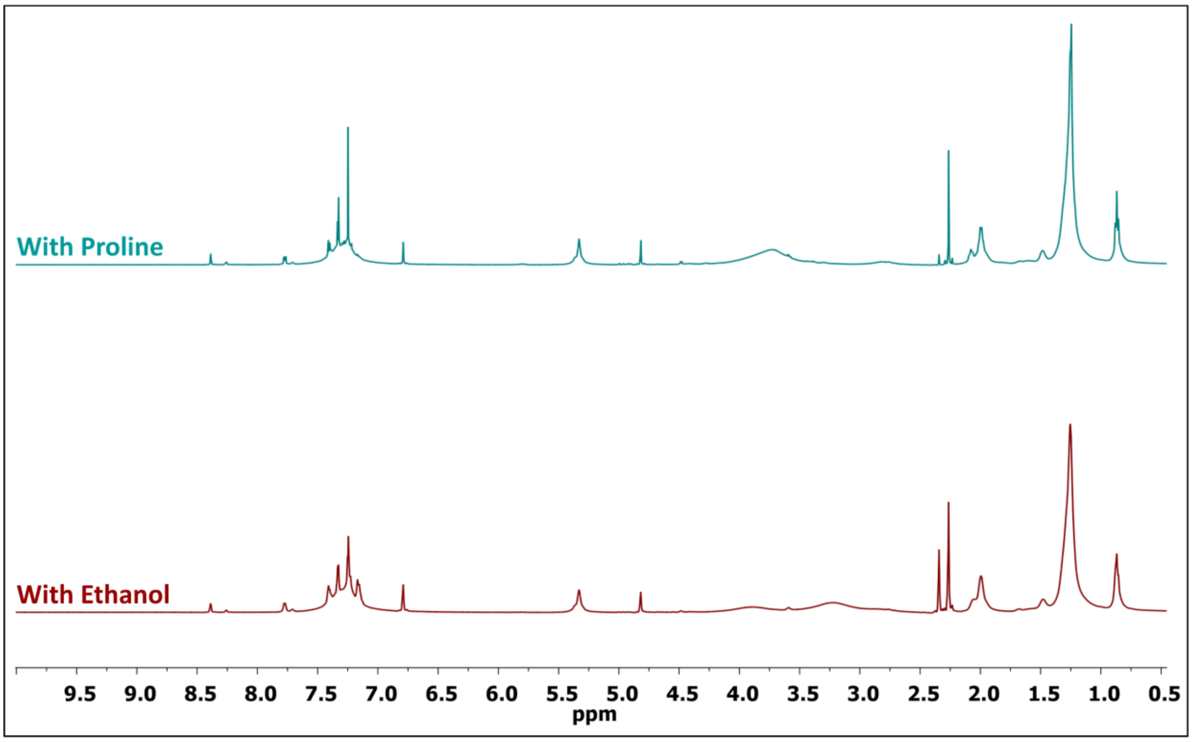

Figure S9. ^{1}H NMR spectrum of control experiment performed in presence of ethanol (hole scavenger and proline ($O_2^{\bullet-}$ scavenger) keeping the other reaction conditions unchanged.

S8. Time-dependent Product Yield of Photocatalytic Reaction

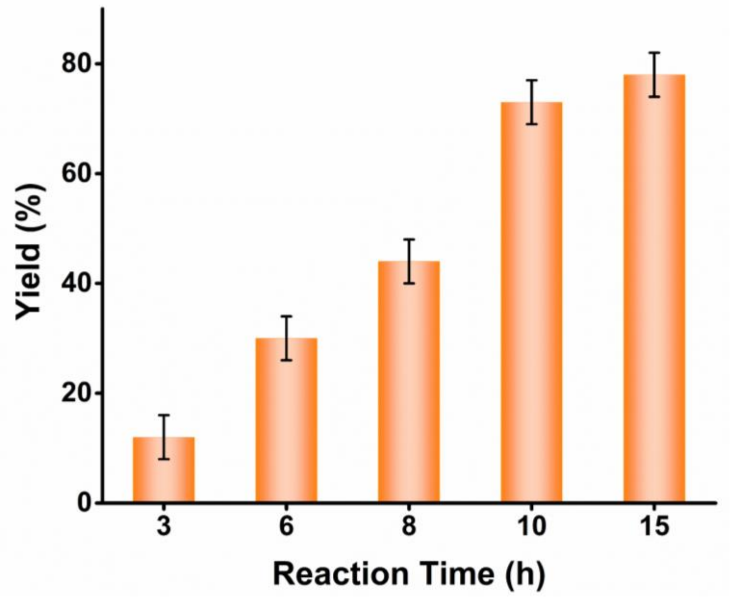

Figure S10. Time dependent yield of the standard reaction keeping the other reaction conditions constant.

S9. EPR study

To the standard reaction mixture i.e., a colloidal solution of $CsPbBr_3$ NCs (~ 6 μM, 0.4 mL) and benzylamine (60 μL, 1M) in toluene, DMPO (3×10^{-6} moles) was added and mixed properly. The as prepared reaction mixture was irradiated with visible light for 1 h and transferred to the EPR tube immediately. Further, the reaction mixture was then immediately frozen under liquid N_2 and the spectrum was acquired at 120 K.

S10. Substrate scope and reactant interaction study of photocatalytic oxidative reaction

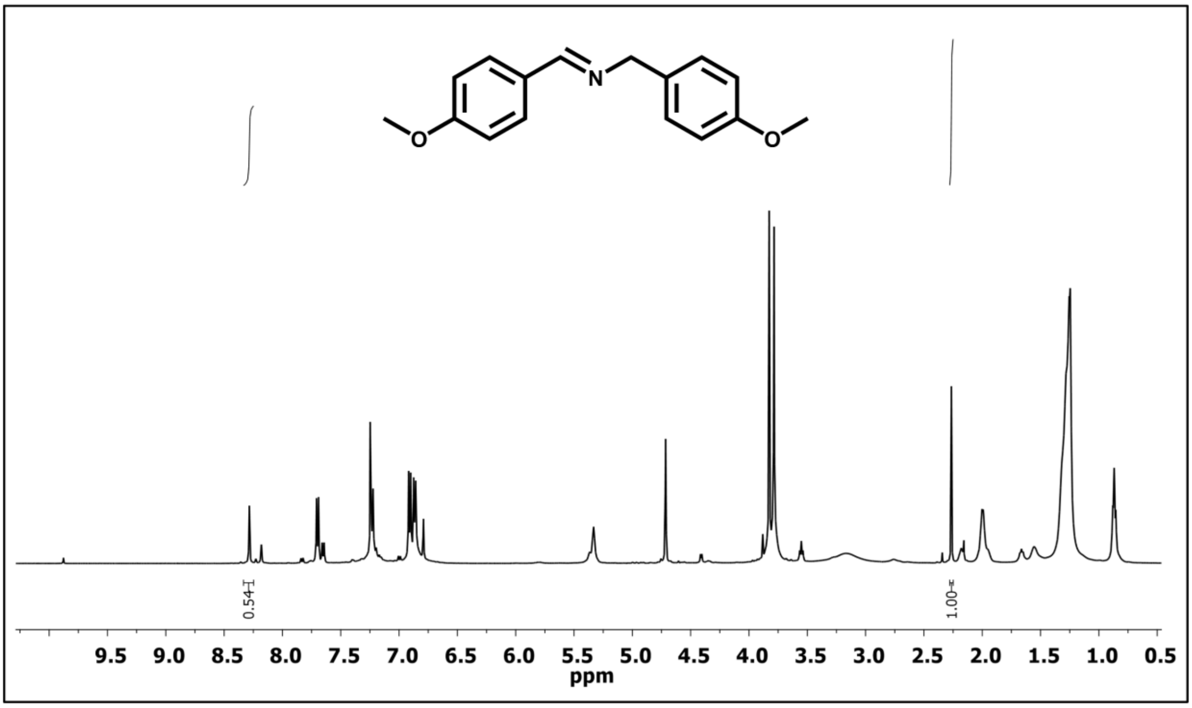

Figure S11. ^{1}H spectrum of N-(4-methoxybenzylidene)-1-(4-methoxyphenyl)methanamine) obtained as a product from coupling of 4-methoxybenzylamine under optimized reaction conditions of standard photocatalytic reaction.

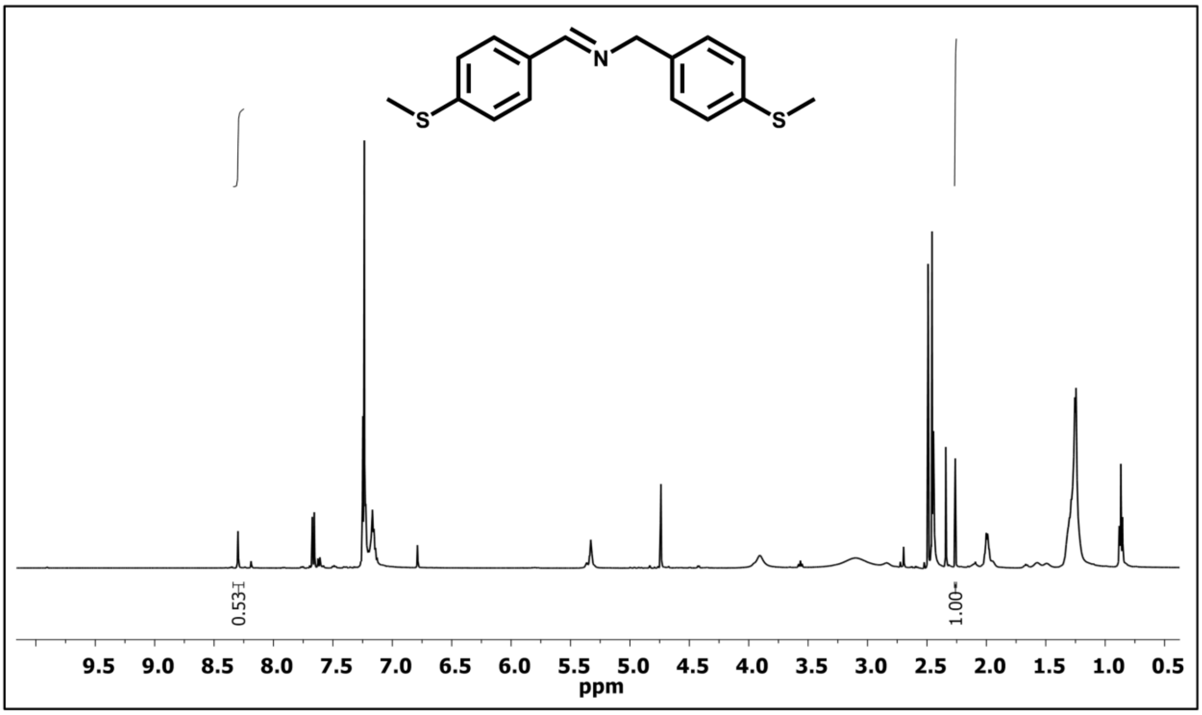

Figure S12. ^{1}H spectrum of N-(4-(methylthio)benzyl)-1-(4-(methylthio)phenyl)methanimine obtained as a product from coupling of 4-(methylthio) benzylamine under optimized reaction conditions of standard photocatalytic reaction. **Note:** We want to mention that we have observed a fraction of product as impurity in the procured 4-(methylthio) benzylamine from Sigma Aldrich. After taking the impurity into account we have observed 38% photocatalytic reaction yield in case of 4-(methylthio) benzylamine (which is mentioned in the main text). Whereas the photocatalytic reaction yield in case of standard benzylamine as a substrate is 69% considering (without $CsPbBr_3$ NCs) reaction conditions yield i.e., 4 %.

Table S1. Reaction yield obtained for the different substrates.

1	Benzylamine	73
2	4-methoxybenzylamine	54
3	4-(methylthio)benzylamine	38

S11. Spectroscopic analysis of interactions between CsPbBr$_3$ NCs and reactant molecules (benzylamine and its derivatives)

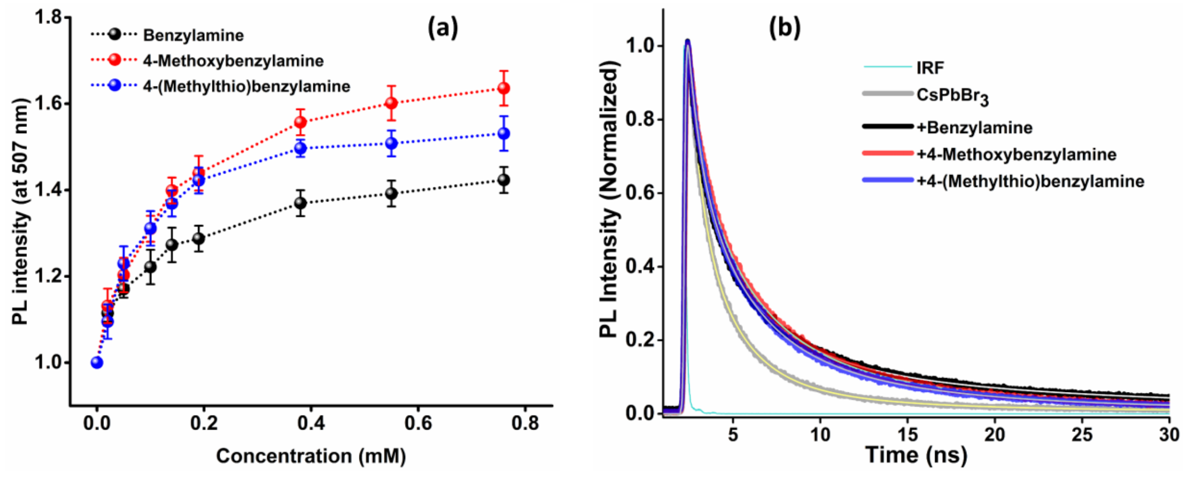

Figure S13. (a) PL intensity (at 507 nm) of CsPbBr$_3$ NCs (22 nM) versus concentration plot for all three different substrates showing the passivation effect (b) Comparative PL lifetime decay of CsPbBr$_3$ NCs in the absence and presence of benzylamine (0.8 mM) and its derivatives (λ_{exc}= 371 nm).

Table S2. Parameters corresponding to PL lifetime decay, fitted to triexponential decay function.

Sample	a_1	τ_1 (ns)	a_2	τ_2 (ns)	a_3	τ_3(ns)	$<\tau>$ (ns)
CsPbBr$_3$	0.44	0.70	0.48	2.32	0.08	8.23	2.08
+ Benzylamine	0.43	0.71	0.43	3.41	0.15	14.31	3.92
+ 4-Methoxy benzylamine	0.31	0.78	0.46	3.09	0.23	9.24	3.79
+4-(Methylthio) benzylamine	0.32	0.65	0.46	2.77	0.22	8.64	3.38

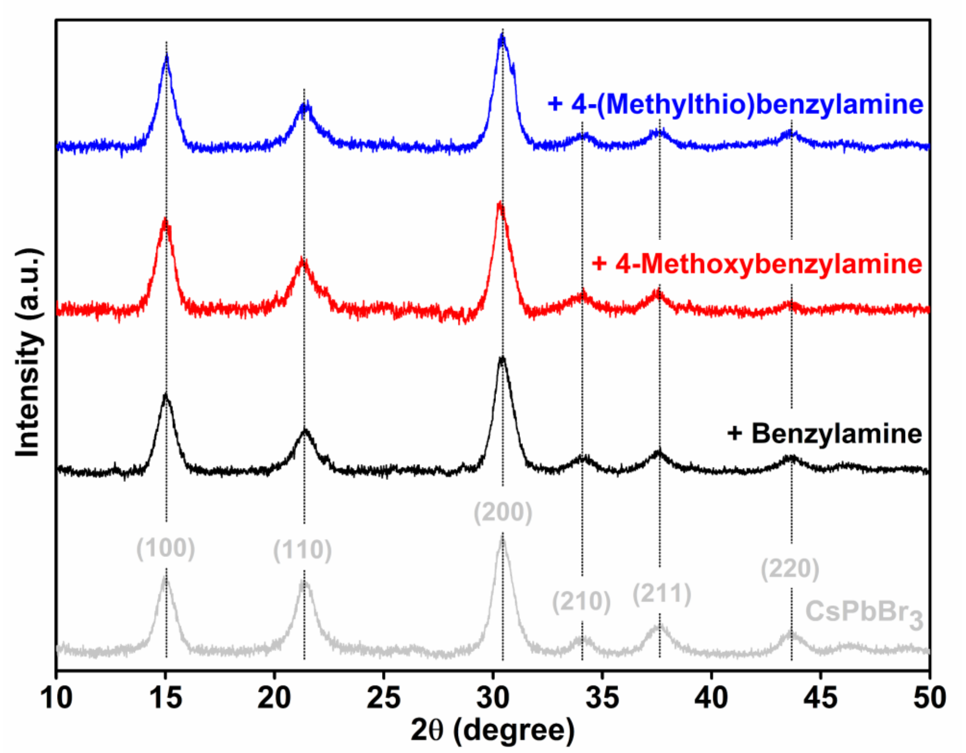

Figure S14. PXRD spectrum of $CsPbBr_3$ NCs before and after treatment with benzylamine, as well as its –OMe and –SMe derivatives, reveals no significant crystallographic changes attributable to different reactant molecules.

FTIR and XPS analysis.

The peaks corresponding to (i) aliphatic H-C= stretch at 917 cm^{-1} and 970 cm^{-1}, (ii) COO^- stretch at 1403 cm^{-1} and 1529 cm^{-1}, (iii) NH_3^+ stretch around 3140 cm^{-1} remain consistent in all the FTIR experiments, indicating the presence of OAm and OAc as the ligand shell for the $CsPbBr_3$ NCs. On the other hand, additional peaks, such as the HNC-H bend (1496 cm^{-1}), C-O stretch (1248 cm^{-1}), and –S–CH_3 stretch (642 cm^{-1}), were observed for $CsPbBr_3$ NCs treated with benzylamine and its –OMe and –SMe derivatives, respectively. These features clearly indicate the presence of reactant molecules on the NC surface. However, they do not completely replace the native ligands.

Further, we carried out XPS measurements for $CsPbBr_3$ NCs with and without the addition of amine reactants. Intriguingly, we observed a significant shift towards higher binding energy (0.1–0.3 eV) and increased broadness of Cs (3d), Pb (4f), and Br (3d) signature peaks on the addition of benzylamine and its derivative reactant molecules, which can be attributed to the interaction of these molecules with the $CsPbBr_3$ NC's surface.[4] Figure S15 represents the comparative FTIR and XPS analysis of the $CsPbBr_3$ NCs.

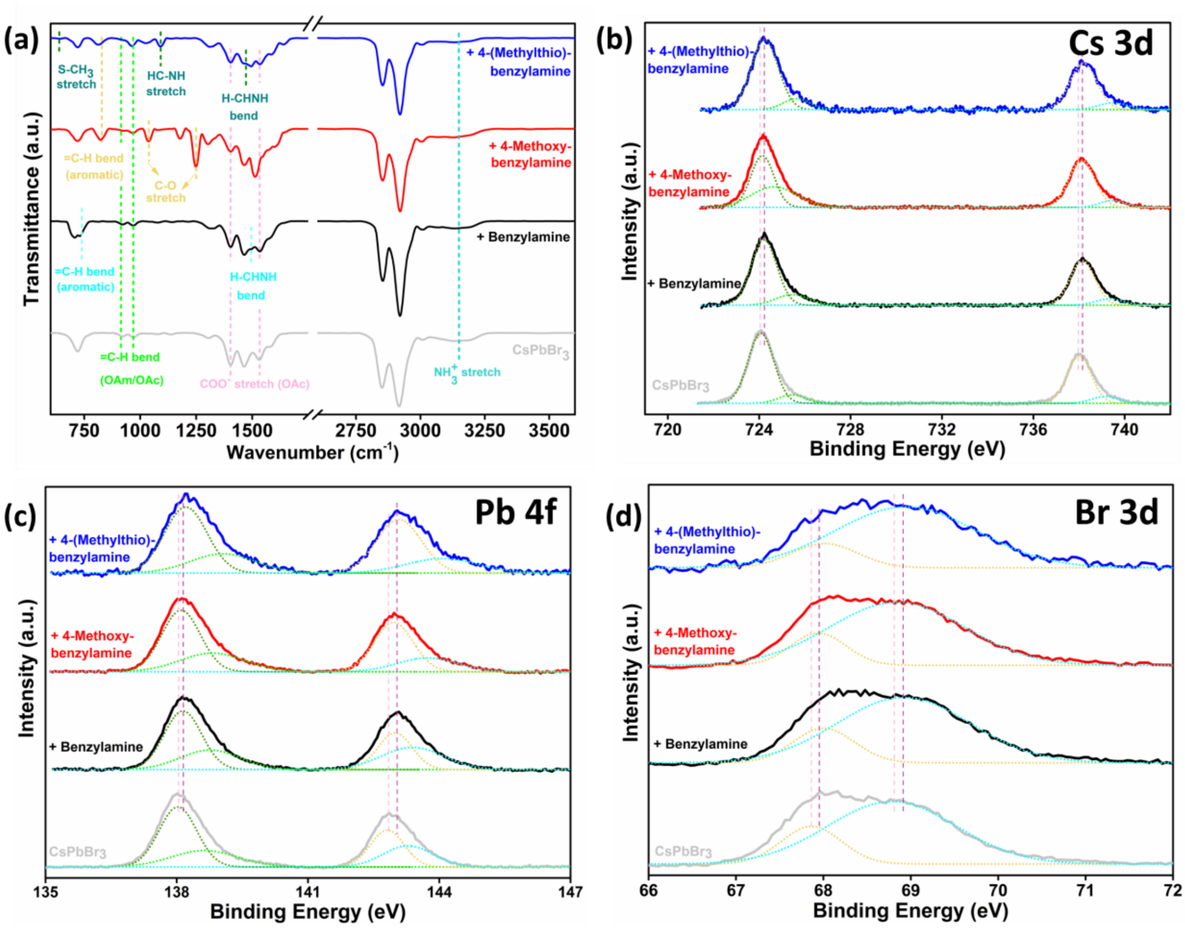

Figure S15. Spectroscopic characterization of $CsPbBr_3$ NCs with amine reactants. (a) FTIR spectrum of $CsPbBr_3$ NCs with and without amine reactant molecules. Deconvoluted high resolution XPS spectrum of (b) Cs 3d (c) Pb 4f, and (d) Br 3d elements obtained from $CsPbBr_3$ NCs with and without reactant molecules. Vertical lines highlight the shift in the binding energy on treatment with amine reactant molecules.

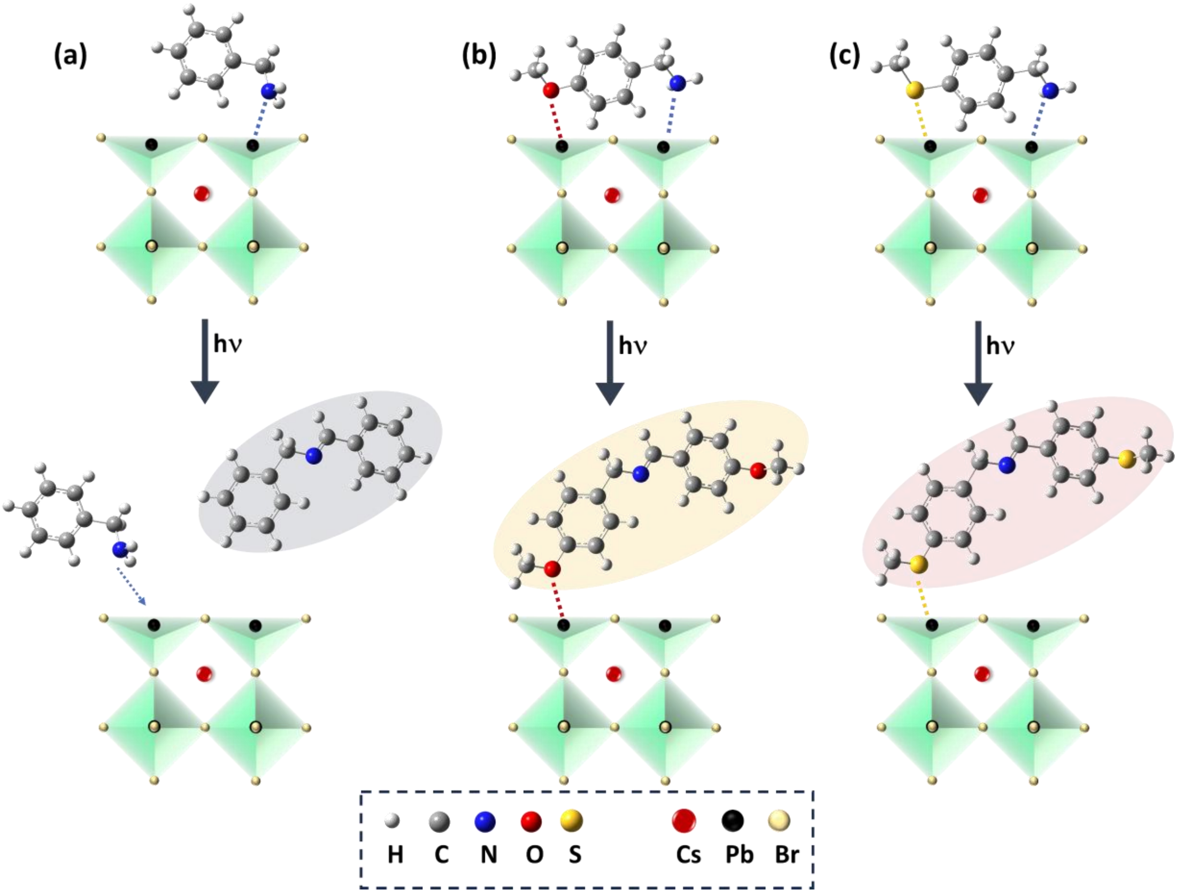

Scheme S1. Schematic showing the plausible interactions between different reactants and $CsPbBr_3$ NC's surface before and after completion of oxidation reaction.

S12. Stability of Catalyst After Photocatalytic Experiments

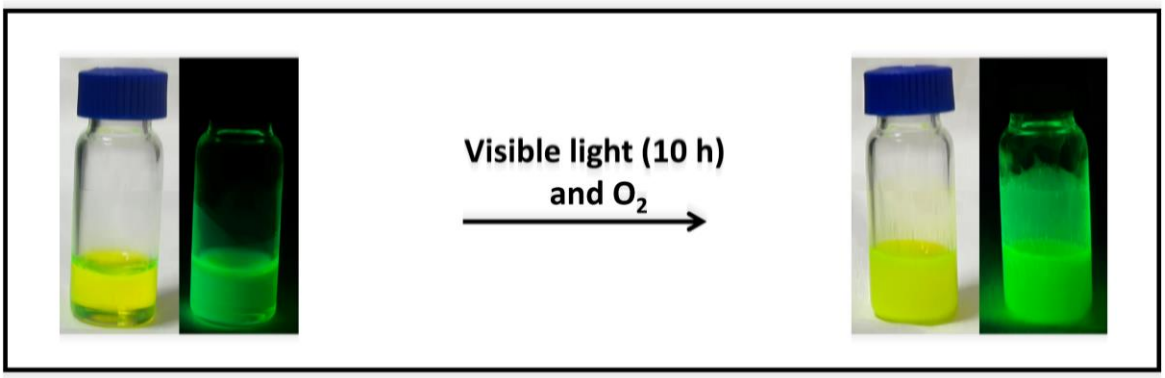

Figure S16. Photographic image of reaction mixture at 0 h and 10 h of visible light exposure in presence of oxygen.

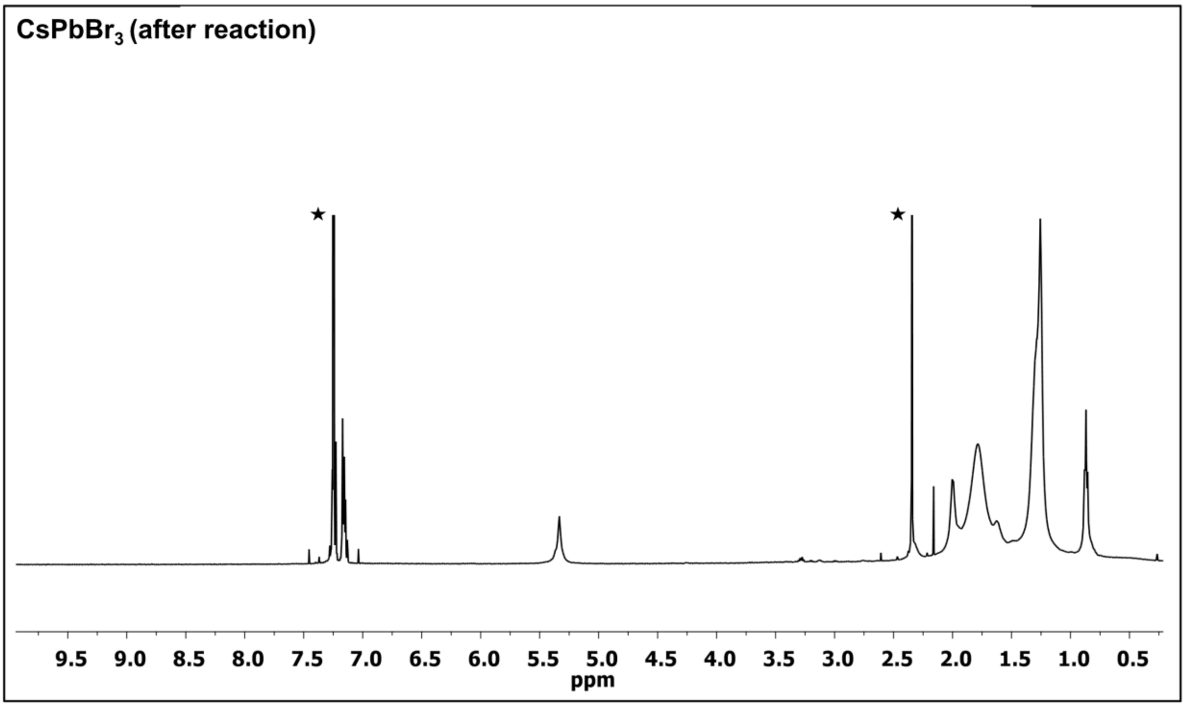

Figure S17. ^{1}H NMR spectrum of CsPbBr$_3$ NCs in CDCl$_3$ after performing the standard reaction.

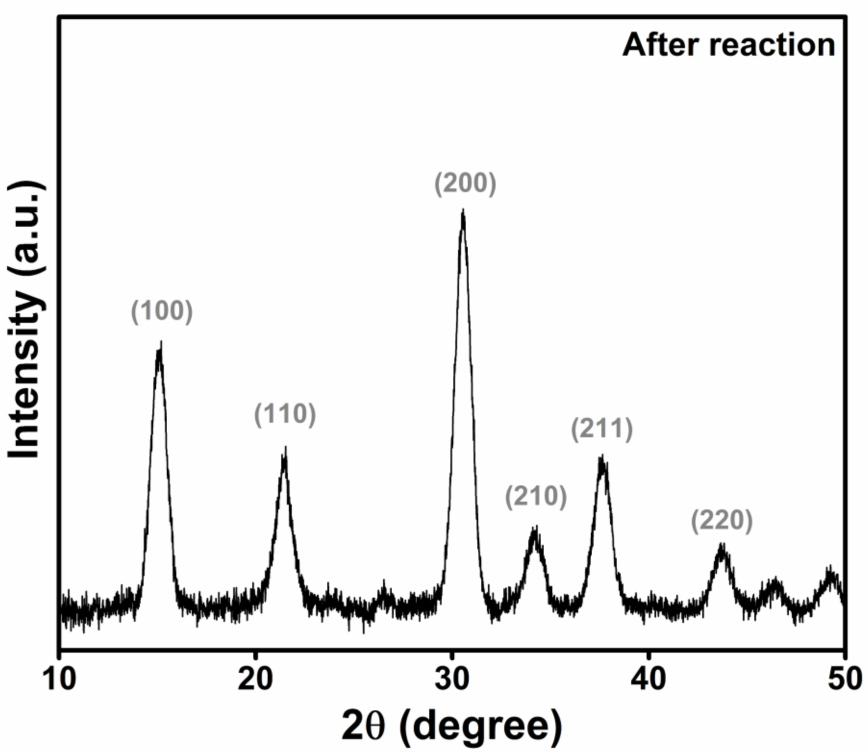

Figure S18. PXRD pattern of CsPbBr$_3$ NCs after undergoing the standard benzylamine oxidation reaction, demonstrating their structural and crystallographic stability throughout the reaction.

Recyclability of $CsPbBr_3$ NCs

After completion of the reaction, the CsPbBr3 NCs were recovered via centrifugation (12000 rpm) using toluene acetone (1:1) mixture with the addition of 10 μL OAm and OAc each to maintain their stability. The NCs were washed twice and redispersed in toluene for further use.

References

1 L. Protesescu, S. Yakunin, M. I. Bodnarchuk, F. Krieg, R. Caputo, C. H. Hendon, R. X. Yang, A. Walsh and M. V. Kovalenko, *Nano Lett.*, 2015, **15**, 3692–3696.

2 J. De Roo, M. Ibáñez, P. Geiregat, G. Nedelcu, W. Walravens, J. Maes, J. C. Martins, I. Van Driessche, M. V. Kovalenko and Z. Hens, *ACS Nano*, 2016, **10**, 2071–2081.

3 J. Chakkamalayath, G. V. Hartland and P. V. Kamat, *J. Phys. Chem. C*, 2021, **125**, 17881–17889.

4 N. Fiuza-Maneiro, K. Sun, I. López-Fernández, S. Gómez-Graña, P. Müller-Buschbaum and L. Polavarapu, *ACS Energy Lett.*, 2023, **8**, 1152–1191.